

^1H NMR, Electron Paramagnetic Resonance, and Density Functional Theory Study of Dinuclear Pentaammineruthenium Dicyanamidobenzene Complexes

Mark L. Naklicki,[†] Serge I. Gorelsky,[‡] Wolfgang Kaim,[§] Biprajit Sarkar,[§] and Robert J. Crutchley^{*,†}

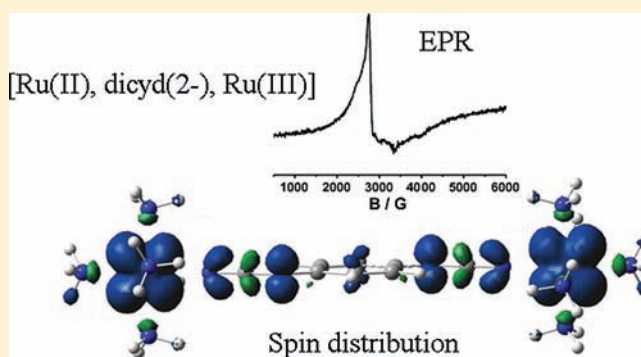
[†]Chemistry Department, Carleton University, Ottawa, Ontario K1S 5B6, Canada

[‡]Centre for Catalysis Research and Innovation, Department of Chemistry, University of Ottawa, Ottawa, Ontario K1N 6N5, Canada

[§]Institut für Anorganische Chemie, Universität Stuttgart, Pfaffenwaldring 55, D-70550 Stuttgart, Germany

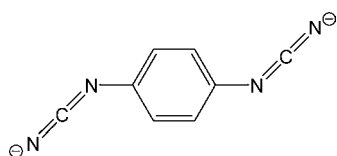
Supporting Information

ABSTRACT: Paramagnetic ^1H NMR and electron paramagnetic resonance (EPR) spectroscopies and density functional theory (DFT) spin density calculations were selectively performed on the $[\{(\text{NH}_3)_5\text{Ru}\}_2(\mu\text{-L})]^{3+, 4+, 5+}$ complexes, where L is 2,3,5,6-tetrachloro-, 2,5-dichloro-, 2,5-dimethyl-, and unsubstituted 1,4-dicyanamidobenzene dianion, to characterize the electronic structure of these complexes. EPR spectra of the $[\{(\text{NH}_3)_5\text{Ru}\}_2(\mu\text{-L})]^{3+}$ complexes in *N,N'*-dimethylformamide at 4 K showed a ruthenium axial signal, and thus the complexes are $[\text{Ru}(\text{II}),\text{L}^{2-}, \text{Ru}(\text{III})]$ mixed-valence systems. DFT spin density calculations of $[\{(\text{NH}_3)_5\text{Ru}\}_2(\mu\text{-L})]^{3+}$ where L = 1,4-dicyanamidobenzene dianion gave mostly bridging-ligand centered spin distribution for both vacuum and implicit solvent calculations, in poor agreement with EPR, but more realistic results were obtained when explicit electrostatic interactions between solute and solvent were included in modeling. For the $[\{(\text{NH}_3)_5\text{Ru}\}_2(\mu\text{-L})]^{4+}$ complexes, EPR spectroscopy showed no signal down to 4 K. Nevertheless, solvent-dependent ^1H NMR data and analysis support a $[\text{Ru}(\text{III}),\text{L}^{2-}, \text{Ru}(\text{III})]$ state. Hyperfine coupling constants (A_c/h) of *trans*- and *cis*-ammine and phenyl hydrogens were determined to be 17.2, 3.8, and -1.5 MHz respectively. EPR studies of the $[\{(\text{NH}_3)_5\text{Ru}\}_2(\mu\text{-L})]^{5+}$ complexes showed a metal-radical axial signal and based on previously published ^1H NMR data, a $[\text{Ru}(\text{IV}),\text{L}^{2-}, \text{Ru}(\text{III})]$ state is favored over a $[\text{Ru}(\text{III}),\text{L}^-, \text{Ru}(\text{III})]$ state.



INTRODUCTION

The bridging ligand 1,4-dicyanamido-benzene dianion (dicyd^{2-})



is redox active and an efficient mediator of antiferromagnetic¹ and resonance exchange² in dinuclear pentaammineruthenium complexes. The reason for this efficiency is the close match in energy between the $\text{Ru}(\text{III})$ $d\pi$ -orbitals and the π -HOMOs of the bridging ligand which permits hole-transfer superexchange. In previous studies, ammine ligands have been replaced with pyridine moieties to decrease the $\text{Ru}(\text{III})$ - $\pi(\text{dicyd}^{2-})$ energy gap and hence increase metal–metal coupling.³ However, at some point, metal $d\pi$ orbitals should become lower in energy the highest occupied orbitals of the bridging ligand. In such case the redox state of the complex would change to correspond to a configuration with a reduced ruthenium ion,

$\text{Ru}(\text{II})$, and radical anion $\text{dicyd}^{\cdot-}$. An example of this situation is the complex $[\{\text{Ru}(\text{tpy})(\text{thd})\}_2(\mu\text{-dicyd})]^+$ where $\text{tpy} = 2,2':6,2''$ -terpyridine and $\text{thd} = 2,2,6,6$ -tetramethyl-3,5-heptanedione monoanion, whose electron paramagnetic resonance (EPR) spectrum showed an organic radical signal, and so the complex oxidation states are best described by $[\text{Ru}(\text{II})\text{-dicyd}^{\cdot-}\text{-Ru}(\text{II})]$.⁴ The redox ambivalence of the dicyd^{2-} ligand has been referred to as noninnocent behavior, and in general the proper description of the electronic structure is fundamental to an understanding of electronic properties of complexes with redox active ligands that have application to biological electronic transfer (ET) processes,⁵ molecular electronics, and molecular computing.⁶ EPR spectroscopy provides the easiest way by which organic radicals can be distinguished from metal radicals, but this requires an observable EPR signal which is not always possible even at liquid helium temperatures. In such instances, paramagnetic NMR spectroscopy can provide unambiguous proof of complex oxidation states.

Received: July 29, 2011

Published: January 5, 2012

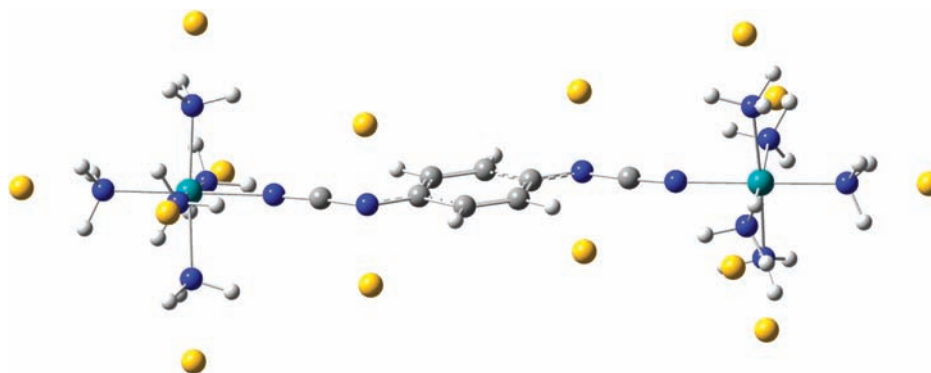


Figure 1. Structure of the $[\{(\text{NH}_3)_5\text{Ru}\}_2(\mu\text{-L})]^{4+}$ complex with the point charges (yellow spheres) shown.

In this study, EPR and ^1H NMR spectroscopies and Density Functional Theory (DFT) methods are selectively applied to the complex ions $[\{(\text{NH}_3)_5\text{Ru}\}_2(\mu\text{-L})]^{3+, 4+, 5+}$, where L = 2,5-dimethyl ($\text{Me}_2\text{dicyd}^{2-}$), unsubstituted (dicyd^{2-}), 2,5-dichloro ($\text{Cl}_2\text{dicyd}^{2-}$), and 2,3,5,6-tetrachloro-1,4-dicyanamidobenzene dianion ($\text{Cl}_4\text{dicyd}^{2-}$), to establish their oxidation states. In addition, the magnitude of antiferromagnetic coupling and hence paramagnetism seen in the $[\{(\text{NH}_3)_5\text{Ru}\}_2(\mu\text{-L})]^{4+}$ complexes can be selectively “tuned” by solvents possessing a range of electron donor properties.^{1b} This in turn, permits a unique opportunity to examine experimentally the relationship between proton isotropic shifts as derived from solution ^1H NMR spectra and the magnitude of spin at constant temperature.

EXPERIMENTAL SECTION

Reagents. Nitromethane- d_3 (99 atom % D, 1% v/v TMS), acetonitrile- d_3 (99.5 atom % D, 1% v/v TMS), acetone- d_6 (99.9 atom % D, 1% v/v TMS and deuterium oxide (99.9 atom % D) were purchased from Aldrich. Dimethylsulfoxide- d_6 (99.9 atom % D) was purchased from Norell Inc. Tetramethylsilane (TMS, 99.9%) and the sodium salt of 2,2-dimethyl-2-silapentane-5-sulfonate (DSS, 99%) were purchased from Aldrich.

Complexes. The ruthenium dimer complexes have been previously prepared as chloride or perchlorate salts.^{1a} In this study, the complexes’ counteranion was usually hexafluorophosphate, however, solubility in nitromethane was significantly improved if tetraphenyl borate was selected. In either case, the appropriate complex was metathesized from an aqueous solution of the complex halide salt by the addition of excess NaBPh_4 or NH_4PF_6 .⁷ The mononuclear complex $[(\text{NH}_3)_5\text{Ru}(2\text{-chlorophenylcyanamide})](\text{PF}_6)_2$ was prepared by the addition of NH_4PF_6 to an aqueous solution of the complex bromide salt.^{7,8} $[(\text{NH}_3)_5\text{CoCl}]\text{Cl}_2$ was prepared according to the method of Schlessinger⁹ and converted to a hexafluorophosphate salt by metathesis with NH_4PF_6 in slightly acidic aqueous solution.

Magnetic Studies. ^1H NMR spectra were obtained at 300 K by using a Bruker AMX-400 NMR spectrometer and reference to TMS (0.00 ppm) in nonaqueous solutions and DSS (0.00 ppm) in D_2O solutions. Solution magnetic susceptibility measurements were determined by the Evans method¹⁰ and have been reported previously.^{1b} Special stem coaxial insert tubes (dimensions: 203 mm \times 4 mm OD) with a capillary reference volume of 60 μL (capillary dimensions: 50 mm \times 2.5 mm OD) were made of precision grade Pyrex by the Wilmad Glass company. The Evans method expression¹¹ for mass susceptibility is

$$\chi_g = \frac{-3\Delta f}{4\pi\nu m} + \left[\chi_0 + \frac{\chi_0(d_0 - d_s)}{m} \right] \quad (1)$$

where Δf is the observed frequency shift in hertz (Hz) of the reference resonance; ν is the fixed probe frequency in Hz of the NMR

spectrophotometer; χ_0 is the mass susceptibility in $\text{cm}^3 \text{g}^{-1}$ of the solvent; m is the mass in grams of the complex per cm^3 of solution; d_0 and d_s are the densities in g cm^{-3} of the solvent and solution, respectively. The term in the square brackets is a correction to the solvent’s density and hence diamagnetism because of the addition of solute. The complex concentration for all the solutions studied was 11.0 mM, except in nitromethane where the solubility of the complexes limited the concentration to 1.8 mM. At these concentrations, the solution density is approximated by $d_0 + m$,¹² and the gram susceptibility simplifies to

$$\chi_g = \frac{-3\Delta f}{4\pi\nu m} \quad (2)$$

Molar susceptibility can be calculated

$$\chi_M = M\chi_g - \chi_D \quad (3)$$

where M is the molecular weight of the complex and χ_D is the diamagnetic correction determined from Pascal’s constants.

In our treatment of the magnetic moment of these dinuclear Ru(III) systems, we have ignored orbital angular momentum. Mononuclear Ru(III) complexes possess magnetic moments which range from 1.90 to 2.07 μ_B ,¹³ suggesting only a small contribution from orbital angular momentum. In agreement, the magnetic moment of $[(\text{NH}_3)_5\text{Ru}(2\text{-chlorophenylcyanamide})](\text{PF}_6)_2$ in acetonitrile- d_3 was determined by using the Evans’ method to be 2.05 μ_B . Finally, the solid state temperature dependence of magnetic susceptibility for the $[\{(\text{NH}_3)_5\text{Ru}\}_2(\mu\text{-L})]^{4+}$ complexes could be successfully modeled by using the spin-only Bleaney–Bowers expression.^{1a}

EPR Spectroscopy. EPR spectra of the complexes were recorded in dimethylformamide (DMF) at 4 K by using a Bruker system EMX. A continuous flow cryostat ESR 900 of Oxford Instruments was used for this purpose.

Computational Details. DFT calculations have been performed using the Gaussian 09 program. In all calculations, the spin-unrestricted molecular orbital approximation was employed. Wave function stability calculations were performed to confirm that the calculated wave functions corresponded to the electronic ground state. The structures of all species were optimized using the B3LYP exchange-correlation functional^{14,15} with the DZVP¹⁶ basis set for all atoms unless indicated otherwise. To test the basis set dependence of the results, several calculations were repeated using the triple- ζ basis set (TZVP)¹⁷ on all atoms except Ru (for which the DZVP basis set was kept). Tight SCF convergence criteria (10^{-8} a.u.) were used for all calculations. Harmonic frequency calculations with the analytic evaluation of force constants were used to determine the nature of the stationary points.

Implicit solvent effects (geometry optimization and electronic structure calculations) in water were evaluated using the PCM model¹⁸ with the UFF atomic radii. Water was selected as a solvent to probe the effects of the highly dielectric medium on the electronic structure of the complexes. Explicit solvent–solvent effects were probed by the model calculations where 14 point charges (with the charges from 0.0

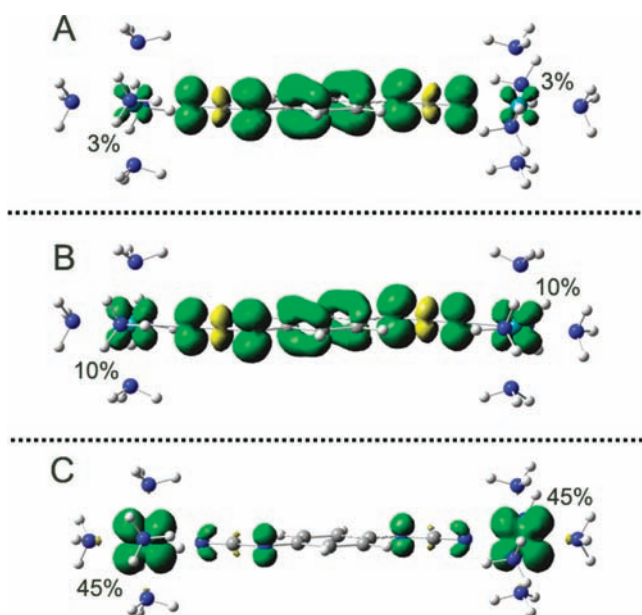


Figure 3. Spin-density distribution (isosurface values of 0.002) $[\{(\text{NH}_3)_5\text{Ru}\}_2(\mu\text{-dicyd})]^{3+}$ in vacuum (a), in dielectric continuum (b), and with explicit electrostatic interactions (c). Green and yellow surfaces show regions with positive and negative spin densities, respectively. NPA-derived atomic spin densities (%) for Ru atoms are shown.

Table 2. Solvent Dependent ^1H NMR Chemical Shifts^a of $[\{(\text{NH}_3)_5\text{Ru}\}_2(\mu\text{-Me}_2\text{dicyd})]^{4+}$ and the Solution Magnetic Moment/Ruthenium ion, 298 K

deuterated solvents	<i>trans</i> NH ₃	<i>cis</i> NH ₃	methyl	phenyl	$\mu_{\text{eff}}/\text{Ru}^b$
nitromethane	6.92	2.96	2.12	7.10	<i>c</i>
acetonitrile	18.75	5.58	3.75	5.27	0.73
acetone	36.87	10.49	5.91	2.91	0.75
DMSO	167.17	43.81	17.11	-8.44	1.16
water	<i>b</i>	<i>b</i>	17.04	-6.58	1.27

^aAll chemical shifts are singlets and gave the correct integration for their assignment; the values in ppm are referenced to TMS (0.00 ppm) in nonaqueous solutions and DSS (0.00 ppm) in D₂O; the complex concentration was 11 mM except in nitromethane where it was 1.8 mM. ^bEvans' method calculation of the magnetic moment per ruthenium ion in B.M. ^cDiamagnetic

hydrogen bonding proximity (2.0 Å) to ammine ligands and the cyanamide groups of the bridging ligand, respectively (Figure 1), to mimic the electrostatic interactions of the complex with polar solvent molecules. The results of these calculations are shown in Figure 3c. The increasing value of point charges from ± 0.1 au to ± 0.5 au increases the spin density localized on the Ru atoms from 7% to 45%. Thus, in the latter case, the spin density is almost entirely localized on the ruthenium ions and the spin density is equally shared between the two metal atoms. The real solvent environment can trap the Ru(III) and Ru(II) ions and, experimentally, $[\{(\text{NH}_3)_5\text{Ru}\}_2(\mu\text{-dicyd})]^{3+}$ has been shown² to be a Class II mixed-valence system²³ with localized charges (i.e., [Ru(III), L²⁻, Ru(II)]). Of course, it is not possible to obtain such spin distribution using calculations with a symmetric $[\{(\text{NH}_3)_5\text{Ru}\}_2(\mu\text{-dicyd})]^{3+}$ structure surrounded by symmetric solvent environment.

^1H NMR Studies. The study of the $[\{(\text{NH}_3)_5\text{Ru}\}_2(\mu\text{-L})]^{3+}$ complexes proved difficult because of the ease of ligand substitution of the pentaamineruthenium(II) coordination

sphere. This is not the case for the $[\{(\text{NH}_3)_5\text{Ru}\}_2(\mu\text{-L})]^{4+}$ complexes and representative spectra of the complex $[\{(\text{NH}_3)_5\text{Ru}\}_2(\mu\text{-dicyd})]^{4+}$ in nitromethane-*d*₃ and dimethylsulfoxide-*d*₆ are shown in Figure 4 and ^1H NMR spectral data for the complexes in various deuterated solvents are compiled

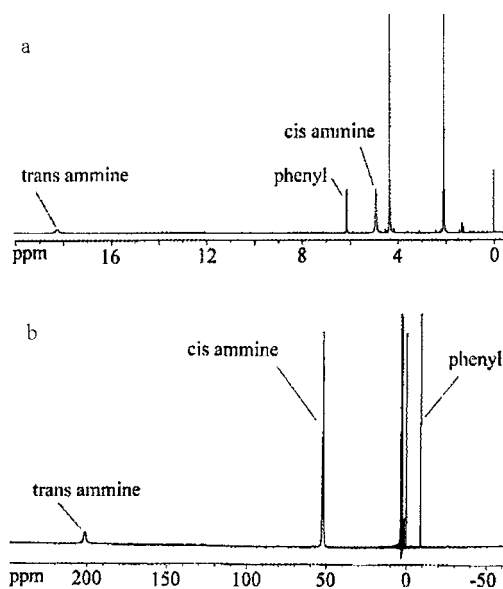


Figure 4. ^1H NMR spectrum of $[\{(\text{NH}_3)_5\text{Ru}\}_2(\mu\text{-dicyd})][\text{PF}_6]_4$ in nitromethane, 1.8 mM (a) and in dimethyl sulfoxide, 11 mM (b).

in Tables 2–5. The spectrum for a given solution consists of 2 to 4 singlet peaks whose assignments were made based on their

Table 3. Solvent Dependent ^1H NMR Chemical Shifts^a of $[\{(\text{NH}_3)_5\text{Ru}\}_2(\mu\text{-dicyd})]^{4+}$ and the Solution Magnetic Moment/Ruthenium ion, 298 K

deuterated solvents	<i>trans</i> NH ₃	<i>cis</i> NH ₃	phenyl	$\mu_{\text{eff}}/\text{Ru}^b$
nitromethane	18.24	4.90	6.12	0.64
acetonitrile	50.53	11.74	1.72	0.79
acetone	76.49	18.12	-1.18	0.88
DMSO	201.72	52.18	-8.99	1.25
water			-8.44	1.35

^aAll chemical shifts are singlets and gave the correct integration for their assignment; the values in ppm are referenced to TMS (0.00 ppm) in nonaqueous solutions and DSS (0.00 ppm) in D₂O; the complex concentration was 11 mM except in nitromethane where it was 1.8 mM. ^bEvans' method calculation of the magnetic moment per ruthenium ion in B.M.

proton integrations. Also included in Tables 1–4 are the solution magnetic moment $\mu_{\text{eff}}/\text{ruthenium}$ values for the complexes. The experimental determination of μ_{eff} for the complexes in nitromethane-*d*₃ were handicapped by poor solubility, and only $[\{(\text{NH}_3)_5\text{Ru}\}_2(\mu\text{-Cl}_4\text{dicyd})]^{4+}$ showed a measurable difference between the reference resonance in the presence and absence of complex.²⁴ Nevertheless, the ^1H NMR spectra of the $[\{(\text{NH}_3)_5\text{Ru}\}_2(\mu\text{-L})]^{4+}$ complexes in nitromethane-*d*₃ showed some evidence of paramagnetic shift, particularly of the *trans*-ammine chemical shift (Table 2–5).

For these antiferromagnetically coupled dinuclear complexes, the increase in μ_{eff} reflects an increase of the triplet excited state population as the exchange constant (*J*) decreases. As shown in a previous study,^{1b} donor–acceptor interactions between the

Table 4. Solvent Dependent ^1H NMR Chemical Shifts^a of $[\{(\text{NH}_3)_3\text{Ru}\}_2(\mu\text{-Cl}_2\text{dicyd})\}^{4+}$ and the Solution Magnetic Moment/Ruthenium ion, 298 K

deuterated solvents	<i>trans</i> NH ₃	<i>cis</i> NH ₃	phenyl	$\mu_{\text{eff}}/\text{Ru}^b$
nitromethane	85.31	20.92	-2.28	0.93
acetonitrile	140.33	34.52	-7.12	1.11
acetone	174.05	43.64	-8.74	1.19
DMSO	245.11	67.13	-8.30	1.38
water			-7.89	1.60

^aAll chemical shifts are singlets and gave the correct integration for their assignment; the values in ppm are referenced to TMS (0.00 ppm) in nonaqueous solutions and DSS (0.00 ppm) in D₂O; the complex concentration was 11 mM except in nitromethane where it was 0.45 mM. ^bEvans' method calculation of the magnetic moment per ruthenium ion in B.M.

Table 5. Solvent Dependent ^1H NMR Chemical Shifts^a of $[\{(\text{NH}_3)_3\text{Ru}\}_2(\mu\text{-Cl}_4\text{dicyd})\}^{4+}$ and the Solution Magnetic Moment/Ruthenium ion, 298 K

deuterated solvents	<i>trans</i> NH ₃	<i>cis</i> NH ₃	$\mu_{\text{eff}}/\text{Ru}^b$
nitromethane	182.20	37.41	1.24
acetonitrile	226.19	48.54	1.30
acetone	246.66	55.03	1.30
DMSO	275.80	72.87	1.42
water			1.86

^aAll chemical shifts are singlets and gave the correct integration for their assignment; the values in ppm are referenced to TMS (0.00 ppm) in nonaqueous solutions and DSS (0.00 ppm) in D₂O; the complex concentration was 11 mM except in nitromethane where it was 0.9 mM. ^bEvans' method calculation of the magnetic moment per ruthenium ion in B.M.

solvent and the ammine ligands decreases Ru(III)-cyanamide resonance exchange and decouples the Ru(III) ions from the bridging ligand. Because the bridging ligand provides the superexchange pathway for antiferromagnetic exchange, the magnetic moment increases with increasing electron-donor properties of the solvent.

In Figure 4b, *cis* and *trans* ammine chemical shifts appear at 52.18 and 201.72 ppm, respectively. This anisotropy in chemical shifts has been noted before in mononuclear pentaammine Ru(III) phenylcyanamide^{20,22} and aquo²⁵ complexes and has been ascribed to a hyperconjugation mechanism which favors the delocalization of spin density from Ru(III) onto the ammine ligand *trans* to the cyanamide group. The data in Tables 2 to 5 show upfield and downfield chemical shifts out of the "normal" diamagnetic region of ^1H NMR spectroscopy, and this occurs because of the coupling of magnetic nuclei with an unpaired electron which gives rise to a chemical shift contribution whose magnitude depends upon the amount of spin density, the extent of coupling, and the molecule's

orientation with respect to the external magnetic field. In solution, rapid molecular motion averages the shift anisotropy, yielding the isotropic shift which can be derived experimentally by taking the difference in shift of a given atom in a paramagnetic compound (observed) and that of the same atom in an analogous diamagnetic compound as shown in eq 4

$$\delta_{\text{iso}} = \delta_{\text{obs}} - \delta_{\text{dia}} \quad (4)$$

In the following analysis, the isotropic shift of the bridging ligand protons was calculated to be the difference between an observed shift and that of the appropriate resonance of the protonated free ligand in DMSO-*d*₆.^{7,26} For the ammine protons, the isotropic chemical shifts were calculated relative to $[\text{Co}(\text{NH}_3)_5\text{Cl}]^{2+}$ ($\delta_{\text{trans}} = 3.12$ and $\delta_{\text{cis}} = 3.75$ ppm).²⁷

Isotropic chemical shifts arise from two main contributions: contact and dipolar shifts

$$\delta_{\text{iso}} = \delta_{\text{con}} - \delta_{\text{dip}} \quad (5)$$

A dipolar shift results from through-space dipolar coupling and is commonly expressed in terms of the anisotropy in *g* values for an axially symmetric system, assuming a point dipole model,²⁸

$$\delta_{\text{dip}} = \left[\frac{\mu_{\text{B}}^2 S(S+1)}{9kT} \right] \left[\frac{(1 - 3 \cos^2 \theta)(g_{\parallel}^2 - g_{\perp}^2)}{r^3} \right] \quad (6)$$

where μ_{B} is the Bohr magneton of the electron, *S* is the total spin, θ is the angle between the principal symmetry axis of the complex and the vector between the metal ion center and the nucleus whose NMR is being observed, and *r* is the distance between metal ion and nucleus. For this study, dipolar coupling occurs from each ruthenium ion with spin derived from eq 7,

$$\mu_{\text{eff}} = g_{\text{av}} \sqrt{S(S+1)} \quad (7)$$

where μ_{eff} is the effective magnetic moment per ruthenium ion and g_{av} is the average *g*-factor. For a given proton, the dipolar coupling from each ruthenium can be determined by using eqs 6 and 7, provided estimates of the *g*-values and geometric values are available. Unfortunately, the $[\{(\text{NH}_3)_3\text{Ru}\}_2(\mu\text{-L})\}^{4+}$ complexes proved to be EPR silent but assuming that the anisotropy in *g*-values is due to a pentaammine ruthenium(III) cyanamido coordination sphere, it is appropriate to average g_{\perp} and g_{\parallel} values respectively of $[\{(\text{NH}_3)_3\text{Ru}\}_2(\mu\text{-L})\}^{3+}$ complexes (Table 1) to yield the estimates: $g_{\parallel} = 2.00$, $g_{\perp} = 2.40$, and $g_{\text{av}} = 2.30$. Computer modeling was used to provide estimates of the appropriate distances and angles in close agreement with crystal structures of similar complexes.^{2,3a,b} Substitution of these values together with eqs 6 and 7 yielded the dipolar shifts δ_{dip} found in Tables 6–8 as well as the contact shifts δ_{con} derived from eq 5. Comparing the magnitude of δ_{dip} to δ_{con} , it is clear that for

Table 6. Isotropic,^a Dipolar, and Contact Shifts of *trans*-Ammine Hydrogens of $[\{(\text{NH}_3)_3\text{Ru}\}_2(\mu\text{-L})\}^{4+}$ in Deuterated Solvents

solvents	L = dicyd ²⁻			L = Me ₂ dicyd ²⁻			L = Cl ₂ dicyd ²⁻			L = Cl ₄ dicyd ²⁻		
	δ_{iso}	δ_{dip}	δ_{con}	δ_{iso}	δ_{dip}	δ_{con}	δ_{iso}	δ_{dip}	δ_{con}	δ_{iso}	δ_{dip}	δ_{con}
NO ₂ CD ₃	15.12	-3.2	18.3	3.8	<i>b</i>	<i>b</i>	82.19	-6.7	88.9	179.08	-11.9	191.0
CD ₃ CN	47.41	-4.8	52.2	15.63	-4.1	19.7	137.21	-9.4	146.6	223.07	-13.0	236.1
Acetone- <i>d</i> ₆	73.37	-6.0	79.4	33.87	-4.4	38.3	170.93	-10.9	181.8	243.54	-13.1	256.6
DMSO- <i>d</i> ₆	198.6	-12.1	210.7	164.0	-10.3	174.3	241.99	-14.7	256.7	276.68	-15.7	292.4

^a $\delta_{\text{iso}} = \delta_{\text{obs}} - 3.12$ ppm. ^bSolution magnetic moment was too small to be measured.

Table 7. Isotropic,^a Dipolar and Contact Shifts of *cis*-Ammine Hydrogens of $[(\text{NH}_3)_5\text{Ru}]_2(\mu\text{-L})^{4+}$ in Deuterated Solvents

solvents	L = dicyd ²⁻			L = Me ₂ dicyd ²⁻			L = Cl ₂ dicyd ²⁻			L = Cl ₄ dicyd ²⁻		
	δ_{iso}	δ_{dip}	δ_{con}	δ_{iso}	δ_{dip}	δ_{con}	δ_{iso}	δ_{dip}	δ_{con}	δ_{iso}	δ_{dip}	δ_{con}
NO ₂ CD ₃	1.15	1.2	0	-0.79	<i>b</i>	<i>b</i>	17.17	2.5	14.7	33.66	4.4	29.3
CD ₃ CN	7.99	1.8	6.2	1.83	1.5	0.3	30.77	3.5	27.3	44.79	4.8	40.0
Acetone-d ₆	14.37	2.2	12.2	6.74	1.6	5.1	39.89	4.1	35.8	51.28	4.9	46.4
DMSO-d ₆	48.43	4.5	43.9	40.06	3.8	36.3	63.38	5.5	57.9	69.12	5.8	63.3

^a $\delta_{\text{iso}} = \delta_{\text{obs}} - 3.75$ ppm. ^bSolution magnetic moment was too small to be measured.

Table 8. Isotropic,^a Dipolar and Contact Shifts of Phenyl Hydrogens of $[(\text{NH}_3)_5\text{Ru}]_2(\mu\text{-L})^{4+}$ in Deuterated Solvents

solvents	L = dicyd ²⁻			L = Me ₂ dicyd ²⁻			L = Cl ₂ dicyd ²⁻		
	δ_{iso}	δ_{dip}	δ_{con}	δ_{iso}	δ_{dip}	δ_{con}	δ_{iso}	δ_{dip}	δ_{con}
NO ₂ CD ₃	-0.84	-0.4	-0.4	0.24	<i>b</i>	<i>b</i>	-9.50	-0.8	-8.7
CD ₃ CN	-5.24	-0.6	-4.6	-1.59	-0.5	-1.1	-14.34	-1.1	-13.2
Acetone-d ₆	-8.14	-0.7	-7.4	-3.95	-0.5	-3.5	15.96	-1.3	-14.7
DMSO-d ₆	-15.95	-1.4	-14.6	-15.30	-1.2	-14.1	-15.52	-1.7	-13.8
D ₂ O	-15.4	-1.7	-13.7				-15.11	-2.3	-12.8

^a $\delta_{\text{iso}} = \delta_{\text{obs}} - \delta_{\text{dia}}$ in ppm; for L = dicyd²⁻, Me₂dicyd²⁻, and Cl₂dicyd²⁻, $\delta_{\text{dia}} = 6.96, 6.86,$ and 7.22 ppm, respectively. ^bSolution magnetic moment was too small to be measured.

these complexes contact shift makes the greatest contribution to the isotropic shift.

A contact shift results from the presence of spin density at the resonating nucleus and can be described by using the spin-only equation^{28,29}

$$\delta_{\text{con}} = \frac{A_C g_{\text{av}} \mu_B S(S+1)}{g_n \mu_n 3kT} \quad (8)$$

where A_C is the hyperfine coupling constant, μ_B is the Bohr magneton of the electron, g_n is the nuclear g -factor, μ_n is the nuclear magneton, k is the Boltzmann constant, and T is temperature. Hyperfine coupling constants are usually determined by measuring the temperature dependence of contact shifts.^{25,30} In this regard, a temperature dependent study (-50 to 25 °C in CD₃CN) of the nearly diamagnetic complex $[(\text{Ru}(\text{NH}_3)_5)_2(\mu\text{-Me}_2\text{dicyd})][\text{PF}_6]_4$ was attempted to see if the singlet ground state could be completely populated and a diamagnetic spectrum obtained. Instead of a diamagnetic spectrum, we observed an increase in the downfield isotropic shift of the ammine protons, presumably because the triplet state is increasingly populated with decreasing temperature. This can only occur if antiferromagnetic exchange decreases with decreasing temperature and, based on the solvent dependent magnetic properties of these complexes, it is suggested that solvent-ammine donor-acceptor interaction must be increasing with decreasing temperature. This complexity prevents the facile evaluation of hyperfine coupling constants by temperature dependent NMR; however, the solvent-dependent magnetic properties of $[(\text{NH}_3)_5\text{Ru}]_2(\mu\text{-L})^{4+}$ at constant temperature provide an alternative method. Expressing the contact shift in terms of μ_{eff} at $T = 298$ K by substituting eq 7 into eq 8, and using $g_{\text{av}} = 2.30$ and the standard values, yields,

$$\delta_{\text{con}} = \frac{A_C \mu_B \mu_{\text{eff}}^2}{g_n \mu_n 3kT g_{\text{av}}} = 1.69 \times 10^{22} A_C \mu_{\text{eff}}^2 \quad (9)$$

For ammine ligands bonded to a given Ru(III) ion in a dinuclear complex, spin is delocalized from the metal ion onto the ammine ligands by the previously mentioned hyper-

conjugation mechanism. The delocalization of spin from the bridged Ru(III) ion to the amines is assumed to be small in which case μ_{eff} is the effective magnetic moment per ruthenium ion. Thus, plots of δ_{con} versus μ_{eff}^2 should be linear with slope proportional to A_C provided A_C is constant for these complexes.³¹ Plots of δ_{con} versus μ_{eff}^2 for *trans* and *cis* ammine hydrogens appear in Figures 5 and 6, respectively, and show linear behavior. The linear-least-squares fits of the data in

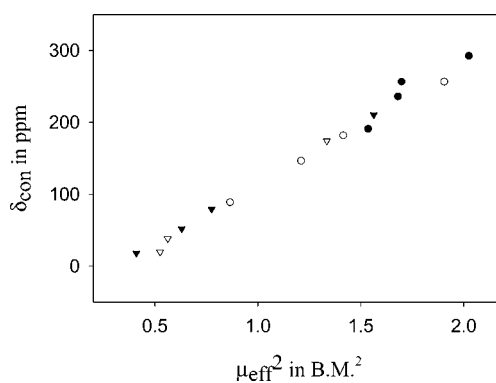


Figure 5. Plot of μ_{eff}^2 versus δ_{con} for the *trans* ammine protons of $[(\text{NH}_3)_5\text{Ru}]_2(\mu\text{-L})^{4+}$ at a complex concentration of 11.0 mM in various solvents. L = Cl₄dicyd²⁻ (●), Cl₂dicyd²⁻ (○), dicyd²⁻ (▼), and Me₂dicyd²⁻ (▽). Data can be found in Tables 2–6.

Figures 5 and 6 gave the hyperfine coupling constants for *trans*- and *cis*-ammine hydrogens of $A_C/h = 15.4$ and 3.4 MHz, respectively.

For the phenyl protons of the bridging ligand, the situation is more complicated as shown in Figure 7. The plot of δ_{con} versus μ_{eff}^2 shows linear behavior, with δ_{con} increasingly negative in magnitude until $\mu_{\text{eff}}^2 > 1.5$, after which δ_{con} becomes smaller in magnitude. This behavior is quite different from that seen for the ammine ligands (Figures 5 and 6) and may be due to an abrupt decrease in spin delocalization onto the phenyl ring.³² The mechanism by which spin can be delocalized onto the dicyd²⁻ bridging ligand is optimum when the π d-orbitals of ruthenium and the π -symmetry orbitals of the cyanamide and

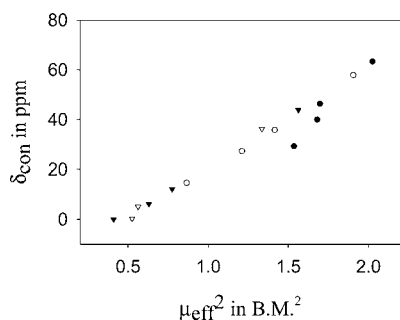


Figure 6. Plot of μ_{eff}^2 versus δ_{con} for the *cis* ammine protons of $[\{(\text{NH}_3)_5\text{Ru}\}_2(\mu\text{-L})]^{4+}$ at a complex concentration of 11.0 mM in various solvents. L = $\text{Cl}_4\text{dicyd}^{2-}$ (●), $\text{Cl}_2\text{dicyd}^{2-}$ (○), dicyd^{2-} (▼), and $\text{Me}_2\text{dicyd}^{2-}$ (▽). Data can be found in Tables 2–5 and 7.

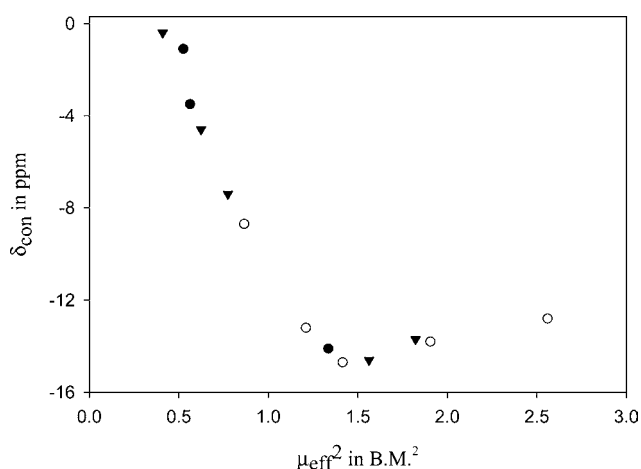


Figure 7. Plot of μ_{eff}^2 versus δ_{con} for the phenyl protons of $[\{(\text{NH}_3)_5\text{Ru}\}_2(\mu\text{-L})]^{4+}$ at a complex concentration of 11.0 mM in various solvents. L = $\text{Me}_2\text{dicyd}^{2-}$ (●), $\text{Cl}_2\text{dicyd}^{2-}$ (○), and dicyd^{2-} (▼). Data can be found in Tables 2–5 and 8.

phenyl ring moieties form a continuous π interaction. The planarity of the bridging ligand and a linear Ru(III)-cyanamide bond are key geometric parameters in this regard. It is suggested that a limit to spin density transferred from Ru(III) to the bridging ligand has been reached at $\mu_{\text{eff}}^2 > 1.5$ because the solvent donor–acceptor interactions that are responsible for the increasing magnetic moment must weaken the linear Ru-cyanamide π bond toward a bent σ -bond conformation. Further increases in solvent donor properties (and hence magnetic moment), serves to increase the σ -bonding only character of the Ru-cyanamide bond and diminishes the effectiveness of the spin delocalization mechanism and so phenyl proton δ_{con} becomes smaller in magnitude. Ignoring the data points higher than $\mu_{\text{eff}}^2 = 1.5$ in Figure 7, gave for the phenyl ring hydrogens an $A_c/h = -1.3$ MHz.

The phenyl ring hydrogen atoms obtain spin density by the polarization mechanism in which π -spin density on the carbon atom (ρ_c^π) induces opposite spin density on the hydrogen atom according to,²⁸

$$A_c(\text{hydrogen}) = \frac{Q\rho_c^\pi}{2S} \quad (10)$$

where Q is the proportionality constant which has a value of approximately -70 MHz.³³ Substituting the appropriate values, ρ_c^π is estimated to be 1.9%. Thus, for the $[\{(\text{NH}_3)_5\text{Ru}\}_2(\mu\text{-L})]^{4+}$

complexes, spin density resides mostly on the ruthenium ions and so are best described by $[\text{Ru(III),L}^{2-}, \text{Ru(III)}]$.

CONCLUSION

EPR spectroscopy of the $[\{(\text{NH}_3)_5\text{Ru}\}_2(\mu\text{-L})]^{3+}$ complexes showed a metal-radical axial signal and thus the complexes are $[\text{Ru(II),L}^{2-}, \text{Ru(III)}]$ mixed-valence systems. DFT calculations of these complexes gave mostly bridging-ligand centered spin for both vacuum and PCM calculations, in poor agreement with experiment, but better results were obtained using an explicit electrostatic model in which the $[\text{Ru(II),L}^{2-}, \text{Ru(III)}]$ state is stabilized. For the $[\{(\text{NH}_3)_5\text{Ru}\}_2(\mu\text{-L})]^{4+}$ complexes, solvent-dependent ^1H NMR data and analysis support a $[\text{Ru(III),L}^{2-}, \text{Ru(III)}]$ state. Hyperfine coupling constants (A_c/h) of *trans*- and *cis*-ammine and phenyl hydrogens were determined to be 17.2, 3.8, and -1.5 MHz, respectively. EPR studies of the $[\{(\text{NH}_3)_5\text{Ru}\}_2(\mu\text{-L})]^{5+}$ complexes showed a metal-radical axial signal and based on the similarity of the previously published ^1H NMR spectrum of $[\{(\text{NH}_3)_5\text{Ru}\}_2(\mu\text{-Me}_2\text{dicyd})]^{5+}$ to those of $[(\text{NH}_3)_5\text{Ru}(\text{pcyd})]^{2+}$ complexes, a $[\text{Ru(III),L}^{2-}, \text{Ru(IV)}]$ state is favored.

ASSOCIATED CONTENT

Supporting Information

XYZ atomic coordinates of optimized structures and composition (%) of frontier β -spin molecular orbitals. This material is available free of charge via the Internet at <http://pubs.acs.org>.

AUTHOR INFORMATION

Corresponding Author

*E-mail: robert_crutchley@carleton.ca.

ACKNOWLEDGMENTS

We are grateful to the Natural Sciences and Engineering Research Council of Canada for financial support.

REFERENCES

- (1) (a) Aquino, M. A. S.; Lee, F. L.; Gabe, E. J.; Bensimon, C.; Greedan, J. E.; Crutchley, R. J. *J. Am. Chem. Soc.* **1992**, *114*, 5130. (b) Naklicki, M. L.; White, C. A.; Plante, L. L.; Evans, C. E. B.; Crutchley, R. J. *Inorg. Chem.* **1998**, *37*, 1880.
- (2) Evans, C. E. B.; Naklicki, M. L.; Rezvani, A. R.; White, C. A.; Kondratiev, V. V.; Crutchley, R. J. *J. Am. Chem. Soc.* **1998**, *120*, 13096.
- (3) (a) Rezvani, A. R.; Bensimon, C.; Crompton, B.; Reber, C.; Greedan, J. E.; Kondratiev, V. V.; Crutchley, R. J. *Inorg. Chem.* **1997**, *36*, 3322. (b) Evans, C. E. B.; Yap, G. P. A.; Crutchley, R. J. *Inorg. Chem.* **1998**, *37*, 6161. (c) Rezvani, A. R.; Evans, C. E. B.; Crutchley, R. J. *Inorg. Chem.* **1995**, *34*, 4600.
- (4) Fabre, M.; Jaud, J.; Hliwa, M.; Launay, J.-P.; Bonvoisin, J. *Inorg. Chem.* **2006**, *45*, 9332.
- (5) Kaim, W.; Schwederski, B. *Coord. Chem. Rev.* **2010**, *254*, 1580.
- (6) Kaim, W.; Lahiri, G. K. *Angew. Chem., Int. Ed.* **2007**, *46*, 1778.
- (7) Naklicki, M. L. Ph.D. Thesis, Carleton University, Ottawa, Ontario, Canada, 1995.
- (8) Crutchley, R. J.; McCaw, K.; Lee, F. L.; Gabe, E. J. *Inorg. Chem.* **1990**, *29*, 2576.
- (9) Schlessinger, G. G. *Inorg. Synth.* **1967**, *9*, 160.
- (10) Evans, D. F. *J. Chem. Soc.* **1959**, 2003.
- (11) (a) Philips, W. D.; Poe, M. *Methods Enzymol.* **1972**, *24*, 304. (b) Schubert, E. M. *J. Chem. Educ.* **1992**, *69*, 62.
- (12) At these concentrations, the amount of solvent displaced by solute is very small, and so the diamagnetism of the solvent is essentially the same in neat solvent and solution.
- (13) Figgis, B. N.; Lewis, J. *Prog. Inorg. Chem.* **1964**, *6*, 173.

- (14) Becke, A. D. *J. Chem. Phys.* **1993**, *98*, 5648.
- (15) Lee, C.; Yang, W.; Parr, R. G. *Phys. Rev.* **1988**, *B37*, 785.
- (16) Godbout, N.; Salahub, D. R.; Andzelm, J.; Wimmer, E. *Can. J. Chem.* **1992**, *70*, 560.
- (17) Schafer, A.; Huber, C.; Ahlrichs, R. *J. Chem. Phys.* **1994**, *100*, 5829.
- (18) Barone, V.; Cossi, M.; Tomasi, J. *J. Comput. Chem.* **1998**, *19*, 404.
- (19) Reed, A. E.; Curtiss, L. A.; Weinhold, F. *Chem. Rev.* **1988**, *88*, 899.
- (20) Mahmoud, L.; Gorelsky, S. I.; Kaim, W.; Sarkar, B.; Crutchley, R. J. *Inorg. Chim. Acta* **2011**, *374*, 142.
- (21) Chiu, W.-H.; Peng, S.-M.; Che, C.-M. *Inorg. Chem.* **1996**, *35*, 3369.
- (22) Naklicki, M. L.; White, C. A.; Kondratiev, V. V.; Crutchley, R. J. *Inorg. Chim. Acta* **1996**, *242*, 63.
- (23) Robin, M. B.; Day, P. *Adv. Inorg. Chem. Radiochem.* **1967**, *10*, 247.
- (24) The digital resolution of the Bruker AMX-400 NMR spectrometer was between 0.3 and 0.5 Hz depending on sweep width.
- (25) McGarvey, B. R.; Batista, N. C.; Bezerra, C. W. B.; Schultz, M. S.; Franco, D. W. *Inorg. Chem.* **1998**, *37*, 2865.
- (26) Aquino, M. A. S. Ph.D. Thesis, Carleton University, Ottawa, Ontario, Canada, 1991.
- (27) Bramley, R.; Creaser, I. I.; Mackey, D. J.; Sargeson, A. M. *Inorg. Chem.* **1978**, *17*, 244.
- (28) (a) Drago, R. S. *Physical Methods for Chemists*, 2nd ed.; Saunders College Publishing: Ft. Worth, TX, 1992. (b) Bertini, I.; Turano, P.; Vila, A. J. *Chem. Rev.* **1993**, *93*, 2833. (c) *Biological Magnetic Resonance, Vol. 12, NMR of Paramagnetic Molecules*; Berliner, L. J., Reuben, R., Eds.; Plenum Press: New York, 1993. (d) Bertini, I.; Luchinat, C. *NMR of Paramagnetic Molecules in Biological Systems*; Benjamin Cummings: Menlo Park, CA, 1986. (e) Bertini, I.; Luchinat, C. *NMR of Paramagnetic Substances*; Elsevier: Amsterdam, The Netherlands, 1996.
- (29) Eq 8 is valid for pure spin states but as the dinuclear complex is in singlet–triplet equilibrium only a fraction of the complex is responsible for the isotropic shift. Strictly speaking both the left and the right sides of eq 8 should be divided by this fraction.
- (30) (a) Paul, F.; Bondon, A.; da Costa, G.; Malvolti, F.; Sinbandhit, S.; Cador, O.; Costuas, K.; Toupet, L.; Boillot, M.-L. *Inorg. Chem.* **2009**, *48*, 10608. (b) Cremer, C.; Burger, P. *J. Am. Chem. Soc.* **2003**, *125*, 7664.
- (31) Average A_c because slight variation is expected between the complexes.
- (32) This assumes that the hyperfine coupling constants of the phenyl protons for the complexes are approximately the same
- (33) (a) ref 27, p. 516. (b) La Mar, G. N. In *NMR of Paramagnetic Molecules*; La Mar, G. N., Horrocks, W. D., Jr.; Holm, R. H., Eds.; Academic Press: New York, 1973; p 113.